A Distributed Model of Four-Port Monolithic Transformer

Dong Ho Lee, Sangsoo Ko, Sang-Hoon Jeon[1], Jae-Woo Park[1], and Songcheol Hong

Department of Electrical Engineering and Computer Science (EECS)
Division of Electrical Engineering of Korea Advanced Institute of Science and Technology (KAIST)
373-1, Guseong-dong, Yuseong-gu, Daejeon, 305-701, Republic of Korea
Tel: +82-42-869-8071 Fax: +82-42-869-8560 Email: overclas@eeinfo.kaist.ac.kr
[1]Knowledge*on Inc., 513-37, Eoyang-dong, Iksan, 570-210, Republic of Korea

Abstract **— This paper deals with modeling of a monolithic spiral transformer. The transformer is designed and fabricated as a symmetrical octagonal spiral structure using two-metal layer process on GaAs substrate for input balun applications of 2 GHz and 5 GHz push-pull power amplifiers. A distributed model of the transformer is developed to fit in wide frequency range with four ports. The model includes the skin effect which describes increase in series resistance with frequency. Six different sets of two-port s-parameters are measured to obtain full characteristics of the four-port transformer while the other two ports are shorted to ground. The model is validated with measurement results in 100 MHz to 6 GHz.**

I. Introduction

Monolithic transformers have found more usage in MMICs and RF circuits. One reason of the increasing demand is led by baluns for differential circuits [1][2], which withstand common noise and even harmonics. Especially, monolithic baluns are necessary for push-pull power amplifiers, which are in class-B or class-D [3][4]. The class-B power amplifiers can achieve higher efficiency and linearity against conventional class-AB power amplifiers. Moreover, VCOs using transformer-based LC tank shows good performance in monolithic VCOs [5].

Using previous simple models, it is hard to fit four-port characteristics simultaneously. From previously reported works, usually the frequency range is under 5 GHz and only two-port through characteristics are validated.

For accurate modeling, a distributed transformer model is presented. Recently, distributed inductor models are developed to reduce errors [6][7]. The distributed model is more close to physical dimension, and the number of parameters is not large, because the distributed model is using common unit cell parameters. Also, the model includes the skin effect which describes increase in series resistance with frequency.

II. Monolithic Transformer

A spiral symmetric transformer is designed and fabricated using two-metal layer process on GaAs substrate for 2 to 5 GHz applications. The line is a thick metal microstrip line which are stacked up by interconnect metal, airbridge post, and airbridge metal. Thickness of interconnect metal, airbridge post, and airbridge metal are 1.5 μm, 3.5 μm, and 4 μm, respectively. Therefore, the total thickness is 9 μm. This stacked line reduces series line resistance. The turn ratio is 4:3 between primary and secondary windings as shown in Fig. 1. The transformer designed with 340 μm outer diameter, 140 μm internal diameter, 15 μm linewidth, and 5 μm line spacing.

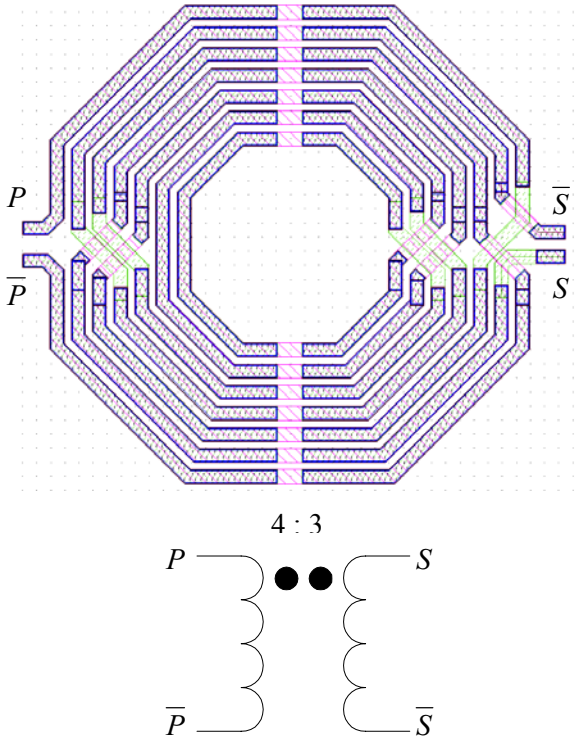

Fig. 1. 4 : 3 symmetric transformer using two-metal layer process.

The symmetric transformer has four outside terminals, which have an advantage to connect to other circuitry [8]. Also, the symmetry obtains center taps easily at the midpoints between the terminals on each winding.

This transformer can be integrated with InGaP/GaAs HBTs. One of the applications is an input balun for push-pull power amplifier. The 4:3 turn ratio achieves the input impedance transformation to high impedance from low impedance of power amplifier input and the turn ratio close to 1:1 acquires high magnetic coupling.

III. DISTRIBUTED TRANSFORMER MODEL

A distributed model is more close to the physical dimension of transformers. Each winding model comprises of four segments as shown in Fig. 2. The number of model parameters is not large, because the distributed model is using common unit cell parameters.

The model includes 8 inductors, but mutual coupling is not whole combination of 8 inductors. The magnetic coupling model is simplified with only four dominant couplings. The coupling between L_1 and L_8 is the same as between L_4 and L_5, and the coupling between L_2 and L_7 is the same as between L_3 and L_6. The dominant couplings are inferred from the physical layout. L_1 is the closest to L_8, L_4 is the closest to L_5, and so on. Also, the parasitic capacitances between two windings are simplified with four dominant capacitances, C_{11} and C_{12}, as the same way of magnetic coupling.

The substrate model is composed of a frequency dependent resistor and a capacitor. The frequency dependent resistor is realized with a capacitor. Five substrate unit models are used for the distributed model of each winding.

Six two-port s-parameter measurements are required for full four-port characterization. The two-port measurements are $P-\overline{P}$, $S-\overline{S}$, $P-S$, $\overline{P}-\overline{S}$, $P-\overline{S}$, and $\overline{P}-S$ when the other two ports are shorted to ground with short bondwires as shown in Fig. 1 and Fig. 5. And the bondwire inductors are deembedded. For right angle calibration, SOLR(Short-Open-Load-Reciprocal through) method is used with Cascade Wincal 3.1 and Cascade 109-531 impedance calibration substrate [10].

The unit segment is initially extracted from $P-\overline{P}$ and $S-\overline{S}$ measurement, which are explained above. Each winding can be considered as a transmission line. Initial parameters of the winding are obtained using RLGC model from a transmission line in Fig. 3 [11]. ABCD parameters are converted from S parameters easily.

$$\begin{bmatrix} A & B \\ C & D \end{bmatrix} = \begin{bmatrix} \cos\gamma l & jZ\sin\gamma l \\ jY\sin\gamma l & \cos\gamma l \end{bmatrix} \tag{1}$$

$$\sqrt{AD} - \sqrt{BC} = e^{-\gamma} \tag{2}$$

$$\frac{B}{C} = \frac{jZ\sin\gamma l}{jY\sin\gamma l} = Z^2 \tag{3}$$

$$R = \mathrm{Re}\{\gamma Z\} \tag{4}$$

$$L = \frac{\mathrm{Im}\{\gamma Z\}}{\omega} \tag{5}$$

$$G = \mathrm{Re}\{\frac{\gamma}{Z}\} \tag{6}$$

$$C = \frac{\mathrm{Im}\{\gamma / Z\}}{\omega} \tag{7}$$

The extracted RLGC parameters are adjusted to distributed parameters, such as

$$R_1 = \frac{R}{4}, \tag{8}$$

$$L_1 = L_2 = L_3 = L_4 = \frac{L}{4}, \tag{9}$$

$$C_{1s} = \frac{C}{5}, \tag{10}$$

$$\text{and} \quad G_{1s}(R_{1s}, C_{1sr}) = \frac{G}{5}. \tag{11}$$

R is an initially fixed parameter, but the other parameters are just initial parameters for fitting optimization. L_1 and L_5 at primary and secondary windings are not free parameters for optimization, and they use only a common coefficient for optimization to keep their physical turn ratio between primary and secondary windings.

Measured R shows the skin effect which describes that R increases with frequency as shown in Fig. 4. The skin effect is modeled as

$$R = \alpha + \beta\sqrt{f} \tag{12}$$

where α is resistance at DC and β is a coefficient of frequency dependent term. The skin effect is also included at the distributed transformer model.

The parameter fitting procedure is accomplished with 6 measurement sets simultaneously.

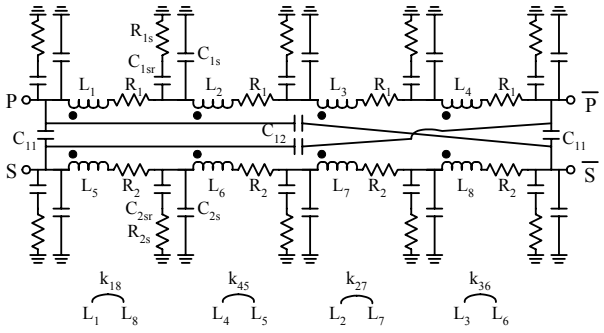

Fig. 2. Distributed transformer model.

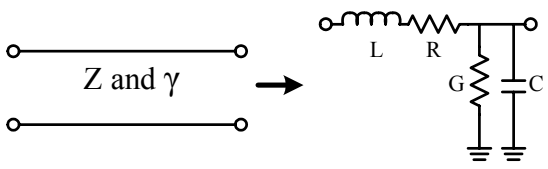

Fig. 3. RLGC model for transmission line.

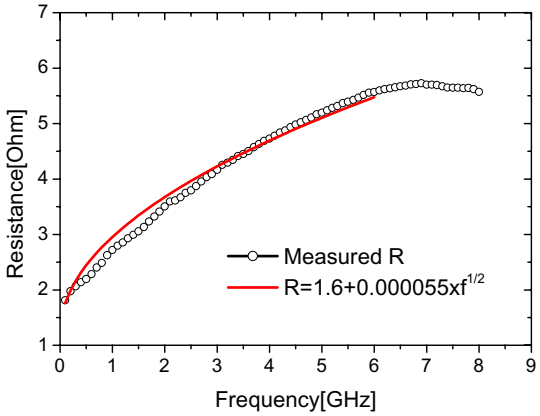

Fig. 4. Series resistance of secondary winding with the skin effect.

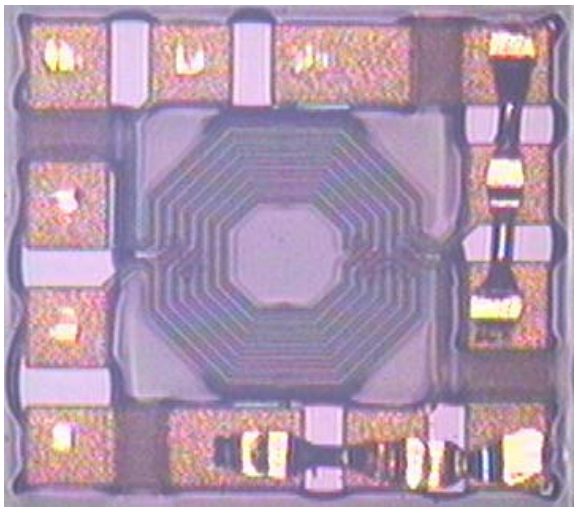

Fig. 5. Implemented 4:3 symmetric transformer with short wire bonding for two-port measurement (667 x 612 μm^2).

IV. Model Verification

It is not easy to fit all six measurement sets simultaneously with a simple model. The distributed transformer model is presented to fit four-port characteristics simultaneously. The model results are shown in Fig. 6. and Fig. 7. At an inverting mode, simulated S11, S22, and S12 are compared with measurement results from 100 MHz to 6 GHz in Fig. 6. And, the results of a non-inverting mode are shown in Fig. 7. Table I shows extracted parameters of the transformer.

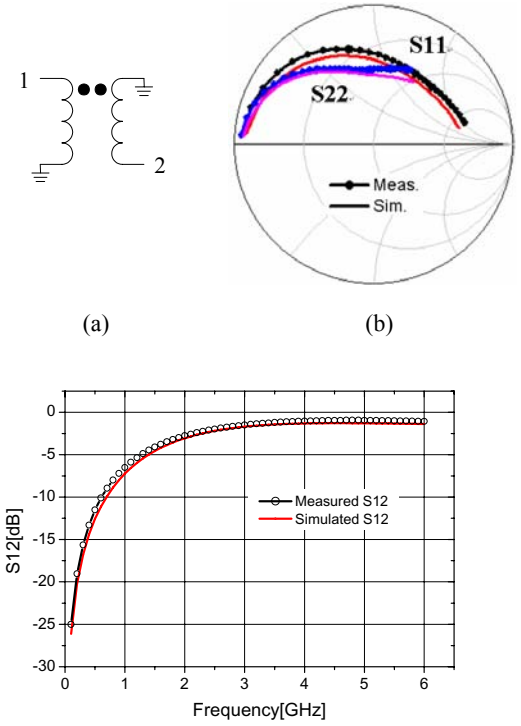

Fig. 6. Inverting mode results. (a) inverting mode schematic, (b) S11 and S22, (c) S12.

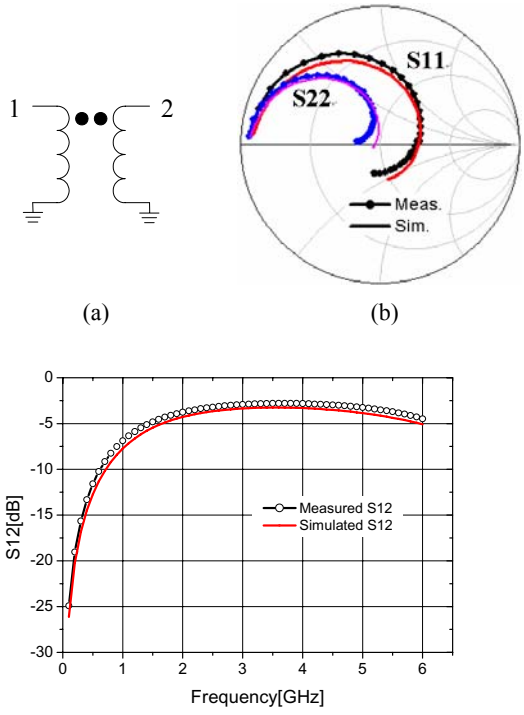

Fig. 7. Non-inverting mode results. (a) non-inverting mode schematic, (b) S11 and S22, (c) S12.

Parameter	Value	Parameter	Value
R_1	$0.4+1.88\times10^{-5}\sqrt{f}$	R_2	$0.3+1.38\times10^{-5}\sqrt{f}$
L_1,L_2,L_3,L_4	0.812 nH	L_5,L_6,L_7,L_8	0.565 nH
C_{1s}	9.93 fF	C_{2s}	9.18 fF
C_{1sr}	158 fF	C_{2sr}	183 fF
R_{1s}	280 Kohm	R_{2s}	1.94 Mohm
k_{18},k_{45}	0.979	k_{27},k_{36}	0.595
C_{11}	240 fF	C_{12}	118 fF

TABLE I
SUMMARY OF EXTRACTED PARAMETERS

V. CONCLUSION

A monolithic transformer is designed and fabricated using two-metal layer process on GaAs substrate for input balun applications of 2 GHz and 5 GHz push-pull power amplifiers. A distributed model of a monolithic spiral transformer is developed to fit with four ports. Also, the model includes the skin effect which describes increase in series resistance with frequency. The extracted model is compared with measurement results in 100 MHz to 6 GHz. The extracted parameters are shown in Table I.

ACKNOWLEDGEMENT

This research was supported by University IT Research Center Project. The authors wish to acknowledge Seungyong Baek for helpful advices.

REFERENCES

[1] J. J. Zhou, and D. J. Allstot, "Monolithic transformers and their application in a differential CMOS RF low-noise amplifier," *IEEE Journal of Solid-State Circuits*, vol. 33, no. 12, pp. 2020-2027, December 2003.

[2] J. P. Maligeorgos and J. R. Long, "A low-voltage 5.1-5.8-GHz image-reject receiver with wide dynamic range," *IEEE Journal of Solid-State Circuits*, vol. 35, no. 12, pp. 1917-1926, December 2000.

[3] V. Paidi, S. Xie, R. Coffie, B. Moran, S. Heikman, S. Keller, A. Chini, S. P. DenBarrs, U. K. Mishra, S. Long, and M. J. W. Rodwell, "High linearity and high efficiency of class-B power amplifiers in GaN HEMT Technology," *IEEE Transactions on Microwave Theory and Techniques*, vol. 51, no. 2, pp. 643-652, February 2003.

[4] W. Simburger, H.-D. Wohlmuth, P. Weger, and A. Heinz, "A monolithic transformer coupled 5-W silicon power amplifier with 59% PAE at 0.9 GHz," *IEEE Journal of Solid-State Circuits*, vol. 34, no. 12, pp. 1881-1892, December 1999.

[5] D. Baek, T. Song, E. Yoon, and S. Hong, "8-GHz CMOS quadrature VCO using transformer-based LC tank," *IEEE Microwave and Wireless Components Letters*, vol. 13, no. 10, pp. 446-448, October 2003.

[6] B.-L. Ooi, D.-X. Xu, and P.-S. Kooi, "A comprehensive explanation on the high quality characteristics of symmetrical octagonal spiral inductor," in *IEEE RFIC Symposium Digest*, Philadelphia, USA, June 2003, pp. 259-260.

[7] A. Ciccazzo, G. Greco, and S. Rinaudo, "A new scalable spice model for spiral inductors in substrate with buried layer," in *Proceedings of RAWCON*, vol. 1, Boston, USA, August 2003, pp. 345-348.

[8] J. R. Long, "Monolithic transformers for silicon RF IC design," *IEEE Journal of Solid-State Circuits,* vol. 35, no. 9, pp. 1368-1382, September 2000.

[9] J. R. Long, "The modeling, charaterization, and design of monolithic inductors for silicon RF IC's," *IEEE Journal of Solid-State Circuits,* vol. 32, no. 3, pp. 357-369, March 1997.

[10] S. Basu, and L. Hayden, "An SOLR calibration for accurate measurement of orthogonal on-wafer DUTs," in *IEEE MTT-S International Microwave Symposium Digest*, vol. 3, Denver, USA, June 1997 ,pp. 1335-1338.

[11] Y. Eo, and W. R. Eisenstadt, "High-speed VLSI interconnect modeling based on S-parameter measurements," *IEEE Transactions on Components, Hybrids, and Manufacturing Technology*, vol. 16, no. 5, pp. 555-562, August 1993.